Bioorganic Chemistry

DOI: 10.1002/ange.200907274

Amide-to-Ester Substitution Allows Fine-Tuning of the Cyclopeptide Conformational Ensemble**

Tommaso Cupido, Jan Spengler, Javier Ruiz-Rodriguez, Jaume Adan, Francesc Mitjans, Jaume Piulats, and Fernando Albericio**

Natural or designed peptide ligands rarely bind to cognate receptors in their most stable conformation when in solution.[1] The receptor, through reciprocal induced fitting,[2] applies pressure on the conformational ensemble of the peptide to select its complementary conformation. Given the flexible nature of the peptides' modular architecture, a bioactive sequence must often be primed for recognition of its target to achieve high binding affinity or specificity. For rational peptide design, cyclization or structure-inducing residues have been successfully used to accomplish ligand preorganization.[3] However, deconvolution of the averaged NMR spectra of strained peptides or other macrocycles had shown that the bound-state conformations are poorly populated in the free uncomplexed state.[4] In small cyclic peptides, the stereochemistry of the backbone, rather than interactions with or among side chains, determines the conformational ensemble by establishing a defined pattern of local torsional preferences.[5] Intramolecular H bonds act on the equilibrium distribution of the conformational ensemble and favor specific conformations.

Thus, we envisioned amide-to-ester substitution or "Ester Scan" as an interesting modification for the peptide backbone, which influences the conformational ensemble as well as its equilibrium distribution; this influence is achieved through modulation of the backbone torsional preferences and H-bonding pattern, respectively.[6]

[*] T. Cupido, Dr. J. Spengler, Dr. J. Ruiz-Rodriguez, Prof. F. Albericio
Institute for Research in Biomedicine (IRB), Barcelona Science Park (PCB) and CIBER-BBN Networking Centre on Bioengineering, Biomaterials and Nanomedicine
PCB Baldiri Reixac 10, 08028 Barcelona (Spain)
Fax: (+34) 93-403-7126
E-mail: tommaso.cupido@irbbarcelona.org
albericio@irbbarcelona.org
Prof. F. Albericio
Department of Organic Chemistry, University of Barcelona
Martì i Franquès 1–11, 08028 Barcelona (Spain)
Dr. J. Adan, Dr. F. Mitjans, Dr. J. Piulats
Biomed Division, Leitat Technological Center Institution, Barcelona Science Park, Baldiri Reixach 15–21, 08028 Barcelona (Spain)

[**] This work was partially supported by CICYT (CTQ2009-07758 and CTQ2008-02856/BQU). The Generalitat de Catalunya (2009SGR 1024, 2009SGR-1472), the Institute for Research in Biomedicine, and the Barcelona Science Park are also acknowledged for support.

Supporting information for this article (experimental details of cyclodepsipeptide syntheses, cellular assays, structure analysis and calculations, characterization of compounds, and MD calculations) is available on the WWW under http://dx.doi.org/10.1002/anie.200907274.

As a model we choose cilengitide (**CIL**), which is an Arg-Gly-Asp (RGD) peptide of sequence cyclo[RGDfNMeV] (see Scheme 1), with well-characterized biological and conformational properties.[7] **CIL** displays nanomolar inhibition of vitronectin binding to the isolated αvβ3 and αvβ5 integrin receptors, and it blocks integrin-dependent adhesion of tumor and endothelial cells to immobilized extracellular matrix (ECM) proteins and reduces angiogenesis and tumor growth in vivo.[8] Modulation of the internal H-bond pattern of nonmethylated **CIL** precursors—achieved by changing the flexibility or the chirality of the backbone—was found to influence the antagonist activity on the vitronectin (VN) and fibrinogen (FB) receptors, and has been proposed to control laminin P1 vs. vitronectin receptor specificity.[9]

We synthesized all five depsi-analogues of the depsipeptide **CIL** (**D1**–**D5**) by stepwise assembling of the linear precursors on 2-CTC resin (Fmoc/*t*Bu strategy) and cyclization in solution. For the introduction of the α-hydroxy acid residues onto the growing peptide chain, their HFA-activated/protected derivatives were used[10] (Scheme 1). For the acylation of the free hydroxy group, DIPDCI/DMAP-activation was used.[11] For conventional peptide cyclization, the optimal site for macrocycle formation is between the Gly (acting as the C terminus) and Asp (acting as the N terminus) residues because Gly cannot epimerize. This strategy was used for the synthesis of parent **CIL**, **D1**, and **D2** depsipeptides with PyBOP/HOAt.[12] The macrolactonization required for the preparation of **D3** was successful with MSNT activation and NMI as the base. For the depsipeptides **D4** and **D5**, certain particularities of the ester bond had to be taken into account. Our attempts to synthesize the linear precursor of **D4** (OGly analogue) starting from OGly as the C terminus, resulted in low yields, and was likely because of cleavage of the ester bond that was mediated by base during repeated treatment with piperidine. Therefore, NMeVal was chosen as the C terminus. For the preparation of **D5**, the cyclization was performed at the (apparently) less attractive position between (D)Phe and NMeVal. Macrolactamization at less hindered sites was impeded by intramolecular nucleophilic attack on the ester bond, which occurred during peptide chain elongation, and eliminated the (D)Phe–NMeVal couple as dioxopiperazine.[13] Given the increased steric demand of the N-terminal NMeVal, we chose the more reactive PyAOP as the coupling reagent and HOAt as the additive.[14]

After cleavage from the solid support, all linear peptide and depsipeptide precursors were obtained in over 85% yield. Head-to-tail cyclization was performed in solution and gave good yields in all cases and, finally, the protecting groups on the side chains were removed using $[Pd(PPh_3)_4]$/phenylsilane

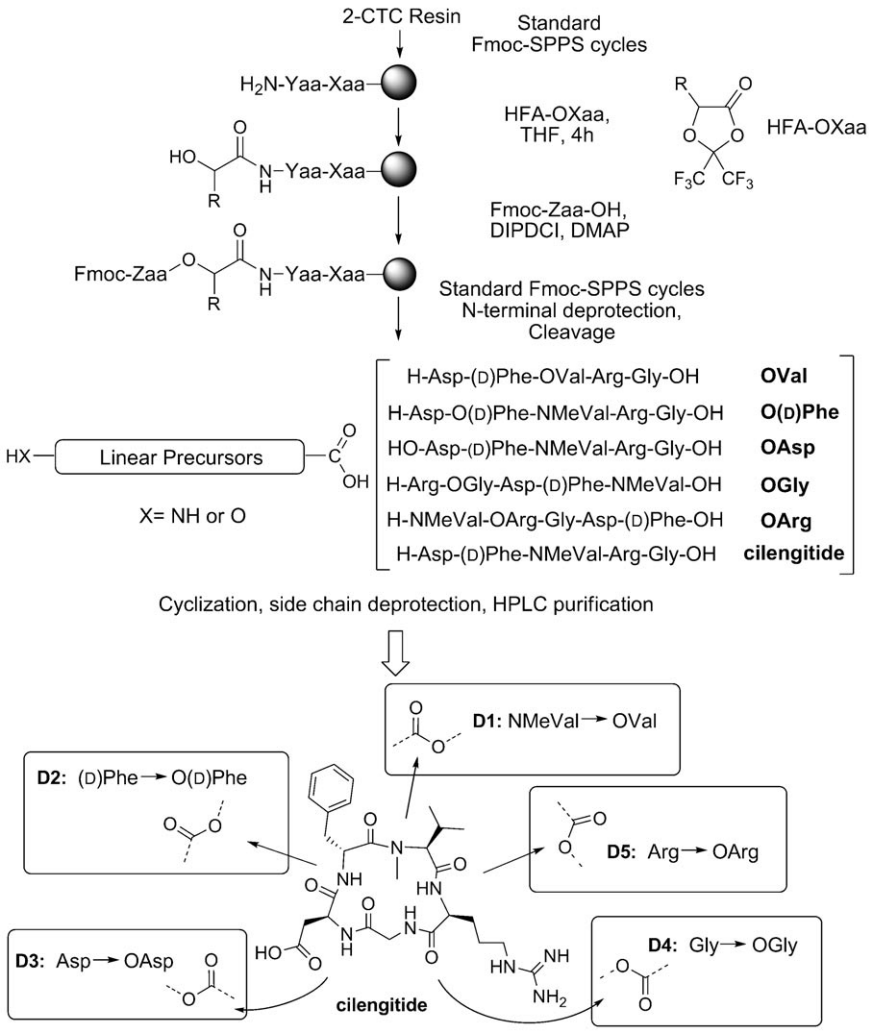

Scheme 1. Synthetic scheme and chemical structures of final RGD cyclodepsipeptides and cilengitide. 2-CTC = 2-chlorotrityl chloride, DIPDCI = 1,3-diisopropyldicarboimide, DMAP = 4-dimethylaminopyridine, Fmoc = 9-fluorenylmethyloxycarbonyl, HFA = hexafluoroacetone, HOAt = 1-hydroxy-7-azabenzotriazole, MSNT = 1-(2-mesitylenesulfonyl)-3-nitro-1,2,4-triazole, NMI = *N*-methylimidazole, PyAOP = 7-azabenzotriazol-1-yloxy)tripyrrolidinophosphonium hexafluorophosphate, PyBOP = 1-benzotriazolyloxytris(pyrollidino)phosphonium, SPPS = solid-phase peptide synthesis.

for the allyl group of **D3**, and TFA/TIS/H_2O for the *t*Bu group of all other pepitides. Finally, purification by HPLC provided the macrocycles **CIL** and **D1**–**D5** in 95 % purity.

For the synthesized compounds, their antagonist activity towards distinct integrin subtypes was tested indirectly as the capacity to inhibit the initial adhesion of a set of cellular lines to the appropriate ECM protein substrate. Adhesion inhibition assays of integrin αvβ3 and αvβ5 were carried out by performing a double-dependent adhesion study of HUVEC endothelial and M21 melanoma cells on VN.[15] Inhibition by **CIL** and **D4** was detected in the high nM range; **D5** was at least three times more active; **D1** showed a two-fold reduction in potency; **D2** was one order of magnitude less potent than cilengitide; **D3** was totally inactive at concentration as high as 30 μM (Table 1). To ascertain whether these differences in potency were a result of the preferential binding of the RGD cyclodepsipeptides to either of the αvβ5 or αvβ3 integrin receptors, we performed an adhesion assay with M21 cells plated on FB (αvβ3-dependent adhesion only), and another with HT29 colon adenocarcinoma cells plated on VN (αvβ5-dependent adhesion only). The same pattern of inhibitory potency described above was observed in these assays. HT29 cells also adhere to fibronectin (FN) through the closely related αvβ6 integrin subtype; neither **CIL** nor depsipeptides **D1**–**D4** inhibited the adhesion of HT29 cells to this substrate (data not shown), in contrast, **D5** showed moderate inhibitory activity (IC_{50} value: 8.64 μM). As expected, neither **CIL** nor any of the depsipeptides inhibited the adhesion of M21 cells to collagen or FN (α2β1- and α3β1-dependent adhesion[16]), thus indicating that they do not antagonize non-αv-containing integrins (data not shown).

Ligand-occupied αvβ3 and αvβ5 receptors down-regulate apoptotic signals from unattached integrins and promote the survival of differentiated endothelial cells.[17] **CIL** antagonizes occupied αvβ3 and αvβ5 integrin and inhibits the proliferation of HUVEC cells plated on purified VN (Table 2). Analogue **D5** displayed an IC_{50} value ten-fold lower than that of **CIL**. Analogues **D4** and **D1** showed inhibitory activity similar to that of **CIL**, whereas **D2** was more than ten-fold less potent. Again **D3** showed no inhibitory activity. As a positive control, we used the anti-αv-integrin monoclonal antibody Mab 17E6.[18]

The conformation of the synthesized compounds in solution was studied by 1D and 2D ^{1}H NMR spectroscopy. The high temperature coefficient of the NH-Arg group, the narrow range on which the $^3J_{HAHN}$ coupling constants were distributed, and a

Table 1: Adhesion inhibition assays of **CIL** and **D1**–**D5**. IC_{50} values are given in μM and the standard deviations are in parentheses.

Peptides	αvβ3 + αvβ5		αvβ3	αvβ5
	HUVEC on VN	M21 on VN	M21 on FB	HT29 on VN
CIL	0.46 (0.10)	0.21 (0.10)	0.32 (0.10)	0.20 (0.04)
D1	0.84 (0.15)	0.45 (0.21)	0.37 (0.10)	0.41 (0.16)
D2	4.32 (0.82)	5.35 (0.75)	5.67 (0.90)	20.51 (3.3)
D3	> 30	> 30	> 30	> 30
D4	0.27 (0.05)	0.19 (0.06)	0.20 (0.10)	0.58 (0.13)
D5	0.18 (0.06)	0.08 (0.02)	0.10 (0.02)	0.06 (0.03)
Mab 17E6	0.001	0.001	0.001	0.0001

Table 2: Proliferation inhibition assay of **CIL** and **D1**–**D5**. IC_{50} values are given in μM and the standard deviations are in parentheses.

Peptide	HUVEC cells	Peptide	HUVEC cells
CIL	0.36 (0.10)	**D4**	0.54 (0.09)
D1	0.34 (0.20)	**D5**	0.04 (0.01)
D2	6.43 (2.4)	**Mab 17E6**	0.00018
D3	>30		

conserved pattern of conformationally relevant NOE interactions (see the Supporting Information for details) suggest that the cyclodepsipeptide analogues of cilengitide retain the overall conformation and side chains topology of the parent cyclopeptide. The time- and ensemble-averaged 3D structures of the synthesized compounds, obtained by simulated annealing (SA) calculations, were generally very similar—with most variability limited to the (D)Phe Φ angle and the Asp Ψ angle (i.e. the tilt angle of the Asp-(D)Phe amide group; see Figure 1 and the Supporting Information). The only significant violation of the NMR constraints was found in the lowest-energy conformation of **D4**, in which the amide plane of Asp-(D)Phe was flipped about 130° with respect to its restrained position, thus suggesting that a conformational equilibrium is occurring in this cyclodepsipeptide analogue. Despite the likeness of their lowest-energy NMR structures, the antagonist potencies of the cyclodepsipeptides on the integrin receptors differed by more than two orders of magnitude.

The observation that the solution (Figure 1; picture to the left of each structure) and the integrin-bound cilengitide structures[19] show different arrangements of the RGD sequence led us to the following hypothesis: divergence in the IC_{50} values for cyclodepsipeptide analogues of cilengitide may result from a differential population of the RGD conformation competent for receptor binding (see the Supporting Information).

We then attempted molecular dynamics (MD) calculations to gain insight into the distributions that make up the averages of the conformational properties, as determined by NMR spectroscopy. Unrestrained simulation trajectories of 22 ns in water were generated using a polarizable force field.[20] The lowest-energy SA conformations were used as starting structures (see the Supporting Information). Cluster analysis of the trajectories obtained by the MD calculations confirmed that **CIL** and RGD cyclodepsipeptides **D1**–**D5** populate similar conformational ensembles. These ensembles are composed of several conformers that differed by the twisting and flipping angles of the planes for amide and ester bonds.

The residence time of single conformers (mostly 10^{-8}–10^{-9} s) and the dynamics of the conformational changes, which are associated with the ester or amide plane flipping, are governed by the torsional preferences of the ester bonds and by the fast (10^{-11} s) formation and disruption of backbone-to-backbone H-bonds. Such an ensemble approach correlates well with the observed NOE interactions and other NMR measurements, and furnishes an explanation for the bioactivity of RGD cyclodepsipeptides. In **CIL**, fast flipping of the amide plane for the Arg-Gly bond defines two major families of conformers, A (including the SA structure) and B (including the integrin bound, and the previously published cilengitide solution structure[7]), which are populated 55% and 35% of the simulation time, respectively (Figure 2a). While in the A or B conformer, **CIL** oscillates between several closely related conformers in fast equilibrium among their torsional forms. Analogue **D2** can be described by an equilibrium of two closely related A and A′ conformers, in which the amide groups of the bioactive RGD sequence are oriented in the same direction (Figure 2a). The two conformers differed by the twist angle of the ester group.

In analogy with **CIL**, the flip of the plane for the Arg-Gly amide group, which converts conformer A into B, was also observed during the MD calculations of **D2**. Conformer B of **D2**, however, appeared less stable and with a shorter residence time than that of its all-amide counterpart (com-

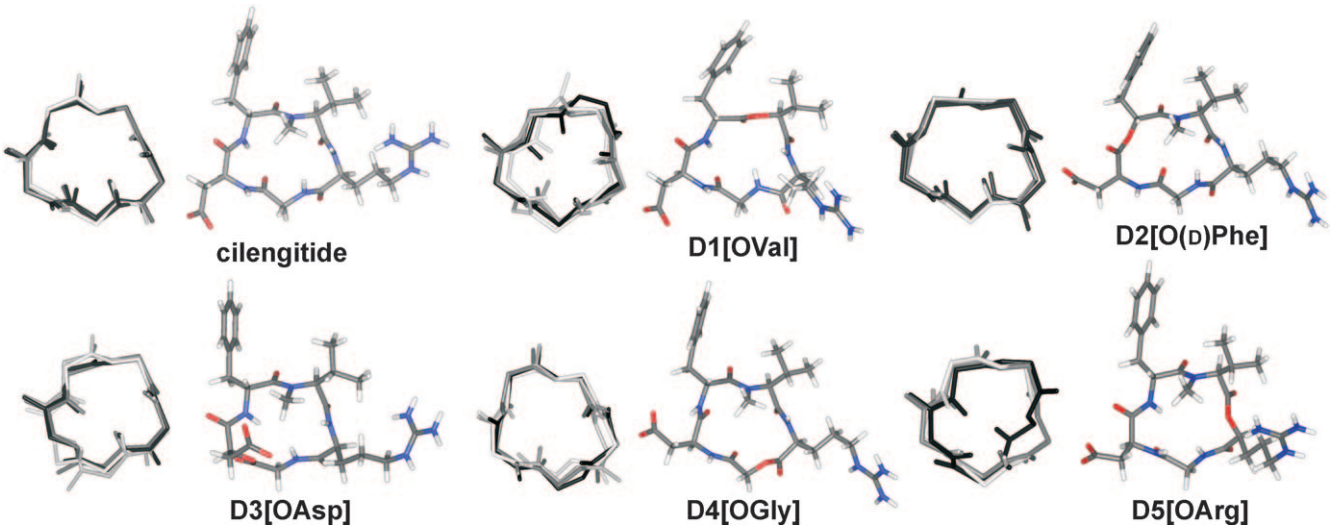

Figure 1. **CIL** and **D1**–**D5** 3D structures obtained by SA. For each macrocycle, the full SA lowest-energy structure is shown, and to its left five backbone conformations representing SA solutions within 3 kcal mol^{-1} are shown (see the Supporting Information for details).

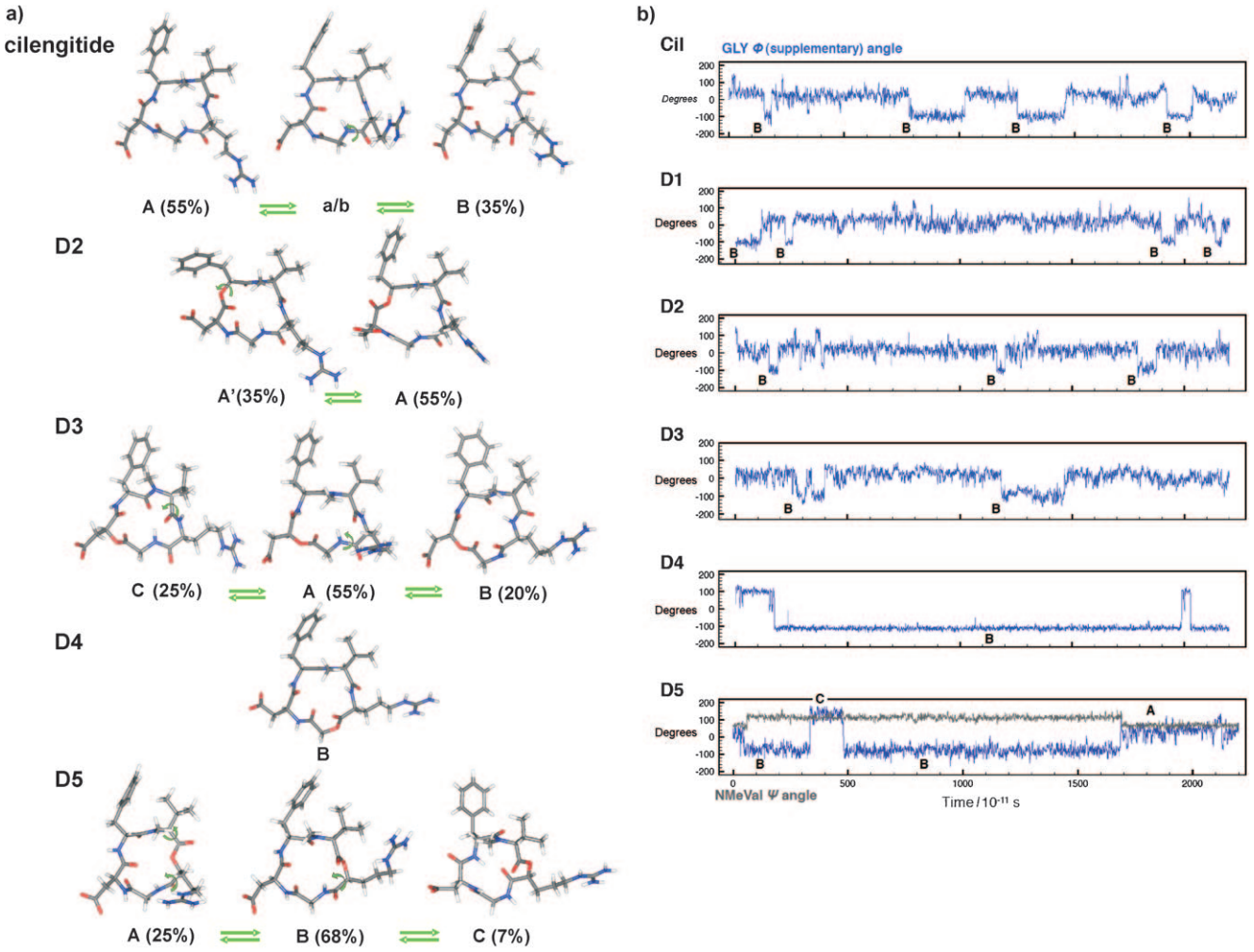

Figure 2. Top: **CIL** and **D1**–**D5** representative conformations and their relative distributions, which were obtained by MD calculations. Arrows indicate the bonds about which rotations (that mediate conformer interconversion) occur. Bottom: Glycine Φ angle variation in **CIL** and **D1**–**D5** during the MD calculations. Abrupt changes indicate Arg-Gly amide group flipping [$A_{(uncompetent)}-B_{(competent)}$ conformer conversion].

pare **D2** with **CIL**; Figure 2b). In **D3**, three conformers rapidly interconvert through uncoupled flipping of the Arg-Gly and the NMeVal-Arg amide groups—where the NMeVal residue displaces from the α region to the β region of the Ramachandran plot[21]—an A conformer (55% populated) converts into a B conformer (20%) by flipping of the former, or into a C conformer (25%) by flipping of the latter. Molecular dymanic calculations of **D4** shows only one conformation analogous to the B conformer of cilengitide, in which the carbonyl oxygen atoms of the Gly and Arg residues have an alternate orientation. The behavior of **D5** in solution can be described by an A conformer converting into a B conformer by simultaneous flipping of the planes for the OArg-Gly amide and the NMeVal-OArg ester bonds. Concomitant transient closure of a seven-membered H-bond arrangement involving the Arg-CO and the HN-Asp moieties contributes to the increased stability of the B conformer in **D5** compared to cilengitide (75% vs. 35% of the simulation time). A unique C conformer is 7% populated in **D5**, and it features an unusual β turn at the Gly-Asp ($i+2, i+1$) couple that is stabilized by a canonical ten-membered H-bond arrangement. For **D3**, **D4**, and **CIL** the upfield shift of the α proton in (D)Phe and the intensity of NOE interactions between the HN-(D)Phe amide proton and the proton in HN-Asp amide or the protons in NMe suggest the existence of a different, significantly populated D conformer, (similar to the lowest-energy structure of **D4** calculated by SA, Figure 1), which originates from flipping of the plane for the Asp-(D)Phe amide group. This motion was occasionally observed only in the **D3** trajectory; for **D4** and **CIL** its dynamics lies outside of our simulation window (between 10^{-8} and 10^{-1} s).

Analysis of the NMR data, the trajectories determined by MD calculations, and the antagonist potencies of cyclodepsipeptide analogues of cilengitide allowed us to formulate a model for the recognition of RGD sequence by the αvβ3 and αvβ5 receptors. In this model an alternate conformation of the Gly-Asp and the Arg-Gly amide groups—pointing in opposite directions—is critical for the formation of ligand–receptor encounter complexes. Subsequent evolution to an high-affinity complex is driven by the formation of intramolecular (GlyCO to HN(D)Phe) and intermolecular

($HNAsp_{cilengitide}$-(β)Arg-$216_{αvβ3\ integrin}$) H-bonds[22] (see the Supporting Information).

In this scenario, the dynamics of the plane flip of the Arg-Gly amide group and the stability of the alternate conformation are key determinants of the binding affinity of RGD cyclopeptides and cyclodepsipeptides to the αv integrins. The conformational preference of the nanomolar antagonist cilengitide is still dominated by an unproductive A conformer that represents the most stable conformation in solution, while the alternate B conformer is only 35% populated (Figure 2a). Accordingly, **D5** had improved potency because the alternate conformation is promoted by the concomitant flip of the plane for the ester bond and stabilized by the formation of a transient backbone H-bond. Analogue **D3**, despite significantly populating the B "alternate" conformer, has no H-bond donor capability at the Asp residue because the NH group is substituted by an oxygen atom, and it lacked any antagonistic activity. Analogue **D2** showed severely diminished antagonist character because it poorly populates the B conformer (Figure 2a).

So far, the use of MD calculations to quantify conformation–activity relationships have been severely limited by the time resolution of state-of-art MD calculations, which is restricted to the μs range, and therefore inadequate to capture some aspects of the conformational flexibility of peptides and proteins. In this study, such an analysis is further complicated by the general inaccuracy of current force fields for the description of nonstandard residues. Indeed, our 22 ns MD calculations failed to completely reproduce the conformational behavior of all RGD macrocycles. As gauged by MD calculations, **D4** mostly adopts the complementary B-receptor conformer, whereas the NMR data showed evidence of a significantly populated D conformer (which remained unexplored during the dynamics experiments). Then, MD calculations led to an overestimation of the population for the B conformer and the antagonist potency of **D4**. According to the presence of the D conformer, **D4** displayed an antagonist potency comparable to that of **CIL** and inferior to that of analogue **D5**.

Taken together these results demonstrate that the targeted application of amide-to-ester substitution or "Ester Scan" in the design of cyclic peptides can be used to fine-tune the backbone conformation and to select a bioactive conformer from the conformational pool. Remarkably, **D5** had three- to ten-fold increased potency with respect to the parent compound, depending on the assay. To the best of our knowledge, **D5** is the most potent small-molecule dual αvβ3 and αvβ5 antagonist discovered to date. Preorganization of flexible peptides into their bioactive conformations has been often achieved by adding local conformational constraints that reduce the allowed backbone Φ and Ψ angles. Herein, we have described a complementary approach which relies on relieving specific conformational constraints by amide replacement with ester groups, thus leading to a targeted reorganization of the internal equilibrium of the conformational ensemble.

Received: December 24, 2009
Published online: March 8, 2010

Keywords: bioorganic chemistry · conformation analysis · depsipeptides · molecular dynamics · NMR spectroscopy

[1] E. Perola, S. P. Charifson, *J. Med. Chem.* **2004**, *47*, 2499.
[2] G. H. Loew, S. K. Burt, *Proc. Natl. Acad. Sci. USA* **1978**, *75*, 7–11.
[3] a) J. D. Tyndall, B. Pfeiffer, G. Abbenante, D. P. Fairlie, *Chem. Rev.* **2005**, *105*, 793; b) R. M. Freidinger, D. F. Veber, D. S. Perlow, J. R. Brooks, R. Sapestein, *Science* **1980**, *210*, 4470; c) R. M. Freidinger, et al., *J. Med. Chem.* **1990**, *33*, 1843 (see the Supporting Information for full citation).
[4] a) S. Horne, C. A. Olsen, J. M. Beierle, A. Montero, M. R. Ghadiri, *Angew. Chem.* **2009**, *121*, 4812; *Angew. Chem. Int. Ed.* **2009**, *48*, 4718; b) J. Jiménez-Barbero, A. Canales, P. T. Northcote, R. M. Buey, J. M. Andreu, J. F. Diaz, *J. Am. Chem. Soc.* **2006**, *128*, 8757.
[5] R. Haubner, R. Gratias, B. Diefenbach, S. L. Goodman, A. Jonczyk, H. Kessler, *J. Am. Chem. Soc.* **1996**, *118*, 7461.
[6] a) E. T. Powers, S. Deechongkit, J. W. Kelly, *Adv. Protein Chem.* **2005**, *72*, 39; b) J. A. Scheike, C. Baldauf, J. Spengler, F. Albericio, M. T. Pisabarro, B. Koksch, *Angew. Chem.* **2007**, *119*, 7912; *Angew. Chem. Int. Ed.* **2007**, *46*, 7766.
[7] M. A. Dechantsreiter, E. Planker, B. Matha, E. Lohof, G. Holzemann, A. Jonczyk, S. L. Goodman, H. Kessler, *J. Med. Chem.* **1999**, *42*, 3033.
[8] a) G. C. Alghisi, L. Ponsonnet, C. Ruegg, *PLoS One* **2009**, *4*, e4449; b) S. M. Weis, D. G. Stupack, D. A. Cheresh, *Cancer Cell* **2009**, *15*, 359; c) Recent results shown that low nM concentrations of cilengitide can promote tumour angiogenesis by agonizing instead of antagonizing the αvβ3 integrin. A. R. Reynolds, et al., *Nat. Med.* **2009**, *15*, 392. (see the Supporting Information for full citation).
[9] a) A. Geyer, G. Müller, H. Kessler, *J. Am. Chem. Soc.* **1994**, *116*, 7735; b) G. Müller, M. Gurrath, H. Kessler, R. Timpl, *Angew. Chem.* **1992**, *104*, 341; *Angew. Chem. Int. Ed. Engl.* **1992**, *31*, 326.
[10] a) F. Albericio, K. Burger, J. Ruiz-Rodriguez, J. Spengler, *Org. Lett.* **2005**, *7*, 597; b) Typically, this coupling step requires 4 hours in THF, whereas the coupling of HFA-(D)OPhe to the N-terminal NMeVal required 48 hours and a higher number of molar equivalents. Glycolic acid (OGly), phenylacetic acid [(D)OPhe], and hydroxyvalerianic acid (OVal) used for the substitution of the Gly, (D)Phe, and NMeVal are commercially available. Appropriately protected malic (OAsp) and argininic acid (OArg) were obtained as described; for OAsp, see: K. Pumpor, E. Windeisen, J. Spengler, F. Albericio, K. Burger, *Monatsh. Chem.* **2004**, *135*, 1427; for OArg, see: T. Cupido, J. Spengler, K. Burger, F. Albericio, *Tetrahedron Lett.* **2005**, *46*, 6733.
[11] O. Kuisle, E. Quiňoà, R. J. Riguera, *Org. Chem.* **1999**, *64*, 8063.
[12] F. Albericio, J. M. Bofill, A. El-Faham, S. A. Kates, *J. Org. Chem.* **1998**, *63*, 9678.
[13] a) B. F. Gisin, R. B. Merrifield, *J. Am. Chem. Soc.* **1972**, *94*, 3102; b) S. Capasso, A. Vergara L. Mazzarella, *J. Am. Chem. Soc.* **1998**, *120*, 1990.
[14] a) Phosphonium salts are preferred ahead of the uronium/aminium salts, because they do not provoke capping of the N terminal function as the latter do, see: F. Albericio, M. Cases, J. Alsina, S. A. Triolo, L. A. Carpino, S. A. Kates, *Tetrahedron Lett.* **1997**, *38*, 4853.
[15] a) D. G. Stupack, X. S. Puente, S. Boutsaboualoy, C. M. Storgard, D. A. Cheresh, *J. Cell Biol.* **2001**, *155*, 459; b) S. Maubant, D. Saint-Dizier, M. Boutillon, F. Perron-Sierra, P. J. Casara, J. A. Hickman, G. C. Tucker, E. Van Obberghen-Schilling, *Blood* **2006**, *108*, 3035.
[16] C. Li, J. B. McCarthy, L. T. Furcht, G. B. Fields, *Biochemistry* **1997**, *36*, 15404.

[17] D. G. Stupack, D. A. Cheresh, *Oncogene* **2003**, *22*, 9022.
[18] F. Mitjans, D. Sander, J. Adan, A. Sutter, J. M. Martinez, C. S. Jaggle, J. M. Moyano, H. G. Kreysch, J. Piulats, S. L. Goodman, *J. Cell Sci.* **1995**, *108*, 2825.
[19] J. Xiong, T. Stehle, R. Zhang, A. Joachimiak, M. Frech, S. L. Goodman, M. A. Arnaout, *Science* **2002**, *296*, 151.
[20] a) R. W. Dixon, P. A. Kollman, *J. Comput. Chem.* **1997**, *18*, 1632; b) V. Babin, J. Baucom, T. A. Darden, C. Sagui, *J. Phys. Chem. B* **2006**, *110*, 11571.
[21] C. M. Wilmot, J. M. Thornton *Protein Engineering, Design and Selection* **1990**, *3*, 479.
[22] L. Marinelli, A. Lavecchia, K. E. Gottschalk, E. Novellino, H. Kessler, *J. Med. Chem.* **2003**, *46*, 4393.

